Diagnostic and Interventional Imaging (2019) **100**, 513—519

ORIGINAL ARTICLE /*Musculoskeletal imaging*

Improved contrast for myeloma focal lesions with T2-weighted Dixon images compared to T1-weighted images

A. Danner[a], **E. Brumpt**[a,b], **M. Alilet**[a], **G. Tio**[c], **P. Omoumi**[d], **S. Aubry**[a,e,*]

[a] *Department of Musculoskeletal Imaging. CHU de Besancon, 25000 Besancon, France*
[b] *Laboratoire d'Anatomie, Université de Bourgogne—Franche-comté, 25000 Besancon, France*
[c] *Clinical investigation center. INSERM CIT808. CHU de Besancon, 25000 Besancon, France*
[d] *Department of Diagnostic and Interventional Radiology. Lausanne University Hospital, 1011 Lausanne, Swizerland*
[e] *Nanomedecine Laboratory inserm EA 4662, Université de Bourgogne—Franchecomté, 25000 Besancon, France*

KEYWORDS
Magnetic resonance imaging (MRI);
Multiple myeloma;
Dixon sequence;
Bone marrow

Abstract
Purpose: The purpose of this study was twofold. First, to compare the contrast between spinal multiple myeloma (MM) focal lesions and surrounding bone marrow obtained on T2-weighted Dixon fat-only MR images to that obtained on T1-weighted spin-echo images. Second, to search for correlation between bone marrow fat fraction assessed by T2-weighted Dixon sequence and International Myeloma Working Group myeloma defining events.
Materials and methods: A total of 39 patients with 112 focal MM lesions were included. There were 25 men and 14 women with a mean age of 68.8 ± 9.8 [SD] years (range: 49-88 years). Contrast between focal MM lesions and surrounding bone marrow was calculated on T1-weighted spin-echo and T2-weighted Dixon (including water-only and fat-only) images. Contrast between focal MM lesions and bone marrow was compared using ANOVA and post-hoc Tukey tests. Correlation between bone marrow fat fraction and myeloma defining events was assessed using Spearman's correlation test.
Results: MM lesion contrast was greater on T2-weighted Dixon ($F(2;93) = 35.10$) than on T1-weighted images ($P < 0.0001$). Greatest MM lesion contrast was achieved with T2-weighted Dixon fat-only (0.63 ± 0.21 [SD]; range: 0.06—0.91) compared to T2-weighted Dixon water-only (0.45 ± 0.20 [SD]; range: 0.07—0.8) ($P = 0.0003$) and T1-weighted (0.23 ± 0.19 [SD]; range: 0.04—0.87) ($P < 0.0001$) images. There were no significant correlations between myeloma defining events and fat fraction.

* Corresponding author.
E-mail address: radio.aubry@free.fr (S. Aubry).

https://doi.org/10.1016/j.diii.2019.05.001

Conclusion: T2-weighted Dixon fat-only images provide greater contrast between MM lesions and adjacent bone marrow than T1-weighted images. The usefulness of a T1-weighted sequence associated to a T2-weighted Dixon sequence has to be determined.

Multiple myeloma (MM) is characterized by autonomous proliferation of monoclonal plasma cells in the bone marrow. The diagnostic criteria used for the diagnosis of MM are 10% or greater clonal bone marrow plasma cells, or an extramedullary plasmacytoma, plus at least one myeloma-defining event present in the extended calcemia renal anemia bone (CRAB) criteria according to the latest recommendations [1]. The International Myeloma Working Group (IMWG) has recommended whole body magnetic resonance imaging (MRI) for work-up of solitary bone plasmacytoma and patients suspected of having smoldering MM [2,3].

Conventional T1-weighted spin-echo sequences and short tau inversion recovery (STIR) have been considered as the most useful tools for the evaluation of bone marrow involvement in routine clinical practice [4,5]. The Dixon technique is a fat-suppression technique based on chemical shift imaging (CSI) [6]. Due to differences in size and polarity in the molecules, protons of fat and water experience different magnetic effects leading to a reduced precessional frequency of fat versus water protons. CSI is based on these differences to produce in-phase (IP) and out-of-phase (OP) images. Decreased signal intensity on the OP images relative to IP images indicates the presence of microscopic fat. Water-only images are obtained by adding the IP and OP datasets, while fat-only images are obtained by subtracting the OP dataset from the IP dataset [7,8]. The benefits of this method are high signal-to-noise ratio images and simultaneous acquisition of images with different contrasts (IP, OP, fat-only and water-only images) [9,10]. Previous studies have shown the non-inferiority or superiority of T2-weighted Dixon sequence over T1-weighted sequence for the detection of bone metastases [11] or the diagnosis of active and chronic sacroiliitis [12].

The purpose of this study was twofold. First, to compare the contrast between spinal MM focal lesions and surrounding bone marrow obtained on T2-weighted Dixon fat-only MR images to that obtained on T1-weighted spin-echo images. Second, to search for correlation between bone marrow fat fraction assessed by T2-weighted Dixon sequence and IMWG myeloma-defining events.

Materials and methods

Study population

Local institutional review board approval was obtained and written informed consent was waived. Patients with a newly diagnosed MM based on the updated IMWG diagnostic criteria [1], and who had undergone a whole spine MRI examination between January 2010 and April 2017 including T1-weighted spin-echo images in the sagittal plane and T2-weighted Dixon images in the sagittal lane with water-only, fat-only, IP, and OP reconstructions were included in this retrospective study. IMWG diagnostic criteria were applied retrospectively to patients who were diagnosed before 2014. Previously treated patients with relapsing disease and no focal MM lesion, or patients with incomplete MRI protocol were excluded. Because of known associations between the following criteria and MM, we excluded patients with: myelodysplasia, history of radiotherapy or chemotherapy. Nineteen patients who previously received specific MM treatment at the time of MRI were not considered for the secondary objective. Fig. 1 summarizes patients inclusion.

A total of 39 patients were included. There were 25 men and 14 women with a mean age of 68.8 ± 9.8 [SD] years (range: 49—88 years). Seven patients (7/39; 18%) had no focal MM lesions and no treatment and 32 patients (32/39; 82%) had a total of 112 focal MM lesions. Of these 32 patients, 19 were under treatment for MM.

Medical records of patients were reviewed by one author (AD). The following IMWG myeloma defining events were collected: serum calcium level (mmol/L), serum creatinine level (μmol/L), serum hemoglobin level (g/dL), clonal bone marrow plasma cell percentage (%), and uninvolved serum free light chain ratio (≤ 99 or > 100).

MRI protocol

MRI examinations were obtained at 3 T in 10 patients (Magnetom Skyra®, Siemens Healthineers) and at 1.5-T in 29 patients (Magnetom Aera®, Siemens Healthineers). The entire spine was acquired in two contiguous sagittal stacks with non-enhanced fast spin-echo T1-weighted and three-point fast spin-echo Dixon T2-weighted sequences of the entire spine from the base of the skull to the last sacral piece. Imaging parameters of the sequences are detailed in Table 1.

Image analysis

Image analysis was performed by a musculoskeletal radiologist with more than 15 years experience (SA) by using **VuePACS®** software (Version 12.1.5.1156, Carestream Health). Focal MM lesions were defined by a low signal on T1-weighted and a high signal on T2-weighted

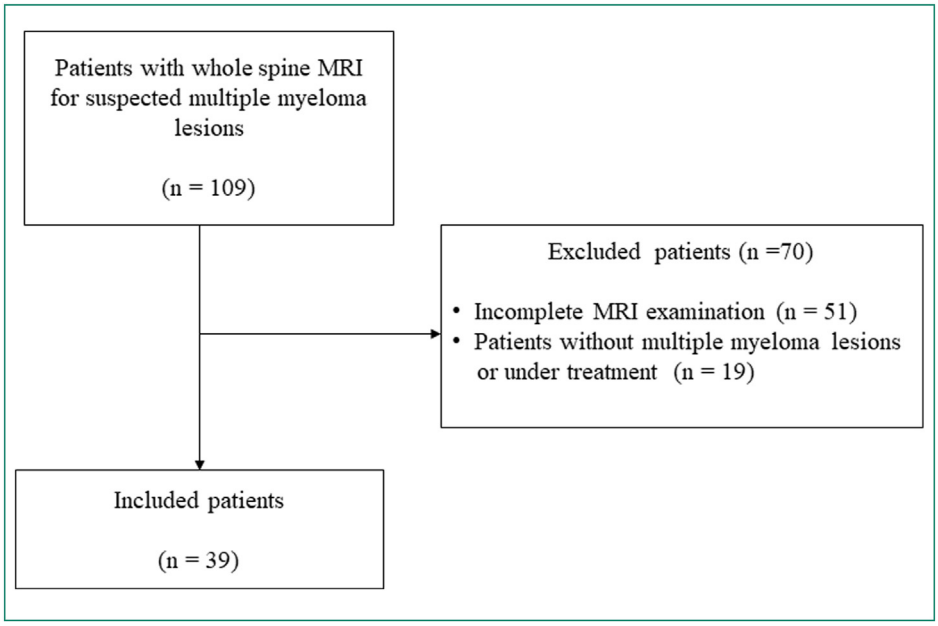

Figure 1. Flowchart shows patients inclusion into the study.

Table 1 Magnetic resonance imaging protocols.

Parameter	MRI sequence			
	T1-weighted		T2-weighted Dixon	
	1.5 T	3 T	1.5 T	3 T
TR (ms)	550	553	4570	4300
TE (ms)	11	10	77	107
Turbo factor	3	3	16	18
Acquisition time	1 min 38 s	1 min 33 s	4 min 31 s	4 min 07 s
Slice thickness (mm)	3	3	3	3
Number of slices	20	21	20	21
Spatial resolution (mm^2)	0.84×0.84	1.04×1.04	0.84×0.84	0.89×0.89

T indicates Tesla; TR indicates repetition time; TE indicates echo time

water-only images and non myelomatous focal lesions such as hemangiomas (characterized by their high signal intensity on T1-weighted images due to fat component), enostosis (which have low signal on every weighting) and cysts (liquid signal) were excluded. Focal lesions within edematous vertebral spine body due to fracture or degenerative changes were also excluded. For each patient, a maximum of 5 focal MM lesions measuring at least 5 mm in diameter was analyzed and for patients with more than 5 focal lesions, the 5 largest ones were selected. There were 7 patients (7/39; 18%) without any lesions, 5 patients (5/39; 13%) with 1 MM lesion, 2 patients (2/39; 5%) with 2 MM lesions, 9 patients (9/39; 23%)with MM 3 lesions, 4 patients (4/39; 10%) with 4 MM lesions, and 12 patients (9/39; 31%) with 5 MM lesions, yielding a total of 112 focal MM lesions.

Mean signal intensity of focal MM lesions and surrounding bone marrow of the same vertebral body (without focal lesion) were calculated by placing round operator-determined regions of interest (ROI) measuring between 5 mm to 15 mm in diameter. The ROIs had a mean surface of 82.7 $mm^2 \pm 75.01$ [SD] (range: 19.6 mm^2—176.6 mm^2). Reference ROIs were placed on T1-weighted images at the center of each focal lesion and on the same slice within adjacent bone marrow at least 1 mm out of the lesion. When present, ''Salt & pepper'' pattern was not excluded from the analysis of bone marrow. In case of absence of focal lesion, ROIs were placed at the center of first to fourth lumbar vertebral bodies. Then, ROIs were copied and pasted at the same location on all other sequences. The contrast between focal MM lesions and bone marrow was calculated using the following equation:

$$\text{Contrast} = \left(\frac{\text{Lesion signal withtin ROI} - \text{Bone marrow signal within ROI}}{\text{Lesion signal withtin ROI} + \text{Bone marrow signal within ROI}}\right)$$

Measurements of bone marrow fat fraction were done by placing ROI as large as possible on L1 to L4 vertebral bodies, except where there was a focal MM lesion. The ROIs were located at least 3 mm far from the endplates and margins of vertebral bodies to prevent effect of partial volume. The fat fraction was assessed according to the following formula [13]:

$$\text{Fat fraction} = \left(\frac{\text{Signal IP} - \text{Signal OP}}{2 * \text{Signal IP}}\right)$$

Statistical analysis

Quantitative variables were expressed as mean ± standard deviation [SD] and range for normally distributed data and median and interquartile range for non-normally distributed data. Qualitative variables were expressed as raw numbers, proportions and percentage. We compared the contrast on T1-weighted, T2-weighted Dixon fat-only and T2-weighted Dixon water-only images, taking into account the patient effect due to multiple lesions. We computed the means and standard deviations of contrast of the different lesions of each patient's sequences, in order then to compare the overall averages of variables between patient's sequences.

Mixed model analysis of variance (ANOVA) was used to compare contrasts of different sequences, and *post-hoc* Tukey tests were used to investigate multiple differences. The Wilcoxon rank-sum test was used to search for a potential link between uninvolved serum free light chain ratio and fat fraction. Spearman's correlation test was used to study the correlation between biological data and fat fraction. Wilcoxon rank-sum test was used to search for possible relationship between the type of MRI (1.5T or 3T) and contrast. A P value < 0.05 was considered statistically significant.

Results

Mixed model ANOVA showed a significant difference in contrast between images when taking into account patient effect (F [2; 93] = 35.10; $P < 0.0001$). Tukey's post-hoc test showed a significant difference between each contrast combination (Table 2). The mean signal intensity of the lesion on T2-weighted Dixon fat-only images was 19.19 ± 27.26 [SD] (range: 1—249), 231 ± 142 [SD] (range: 49—839) on T2-weighted Dixon water-only images and 166 ± 84.91 [SD] (range: 18—442) on T1-weighted images. The contrast was highest on T2-weighted Dixon fat-only images (0.63 ± 0.21 [SD]; range: 0.06—0.91), intermediate on T2-weighted Dixon water-only images (0.45 ± 0.20 [SD]; range: 0.07—0.8), and lowest on T1-weighted images (0.23 ± 0.19 [SD]; range: 0.04—0.87) (Fig. 2). The type of MRI had no significant effect on the contrast ($P = 0.22$).

Results of the correlation analysis between fat fraction and biological data are detailed in Table 3. There was no significant correlation between the biological data of the extended CRAB criteria, and fat fraction. No associations were found between fat fraction and uninvolved serum free light chain ratio ($P = 0.81$). Infiltration and replacement of bone marrow, when present, did not impair the contrast between focal lesions and bone marrow (Fig. 3).

Discussion

Our study found that the contrast on T2-weighted Dixon fat-only images was significantly higher than on T1-weighted images, suggesting that T2-weighted Dixon fat-only may be more efficient to detect focal MM lesions than T1-weighted. Recently, Maeder et al. compared T2-weighted Dixon fat-only to T1-weighted images for the detection of bone metastatic lesions, and showed that the contrast-to-noise ratio was significantly higher with the T2-weighted Dixon fat-only than with T1-weighted [11]. They also showed that diagnostic performance was not significantly inferior with T2-weighted Dixon fat-only than that of a standard protocol including T1-weighted and fat-suppressed fluid-sensitive sequences. Another study demonstrated the higher contrast-to-noise ratio of a T2-weighted Dixon sequence compared to T1-weighted images for depiction of the diagnostic signs of active and chronic sacroiliitis [12]. Bone marrow is formed of approximately 40% yellow and 60% red marrow in the vertebral bodies during the first decade of life. The fatty component of vertebral bone marrow gradually increases with age [14]. On T2-weighted Dixon fat-only images, hypointense focal lesions are better depicted from high—signal intensity fatty background than on T1-weighted images [3,15,16]. As in the case of metastases, the T2-weighted Dixon sequence might be an appropriate alternative to the standard protocol (combination of T1-weighted and fat-suppressed fluid-sensitive sequences) to search for spinal focal MM lesions. Nevertheless, Heynen et al showed that T2-weighted Dixon fat-only images had no significantly different interobserver agreement but were less sensitive than T1-weighted images for the detection of hip and pelvic occult fractures [17]. Due to this specific interest of T1-weighted images, it seems premature to take

Table 2 Comparison of contrast of myeloma focal lesions between different three MRI sequences.

MRI sequence	MRI sequence	*P*-value
T1-weighted 0.23 ± 0.19 [SD]; range: 0.04-0.87	T2-weighted Dixon fat-only 0.63 ± 0.21 [SD]; range: 0.06-0.91	< 0.0001
T1-weighted 0.23 ± 0.19 [SD]; range: 0.04-0.87	T2-weighted Dixon water-only 0.45 ± 0.20 [SD]; range: 0.07-0.8	< 0.0001
T2-weighted Dixon fat-only 0.63 ± 0.21 [SD]; range: 0.06-0.91	T2-weighted Dixon water-only 0.45 ± 0.20 [SD]; range: 0.07-0.8	0.0003

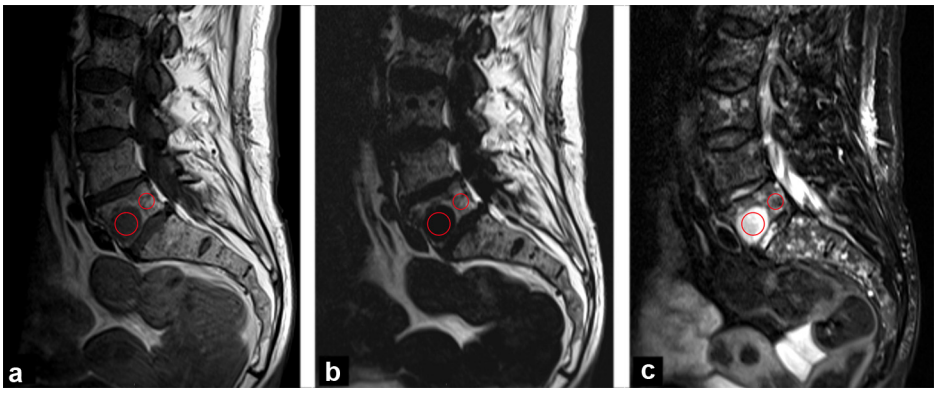

Figure 2. 63-year-old woman with multiple myeloma. a: T1-weighted image in the sagittal plane shows focal myeloma lesion (large circle) of the fifth lumbar vertebra with low signal intensity; b: On T2-weighted Dixon fat-only image, the focal myeloma lesion has no visible signal intensity; c: On T2-weighted Dixon water-only image the focal myeloma lesion has high signal intensity. Better conspicuity of this focal lesion on T2-weighted Dixon fat-only image versus T1-weighted image is supported by a greater contrast between the lesion and surrounding bone marrow (0.84 on T2-weighted Dixon fat-only image versus 0.47 on T1-weighted image).

Table 3 Correlation between biological data of extended CRAB and bone marrow involvement.

	Fat fraction of bone marrow		
	Spearman correlation coefficient	*P*-value	Number of observations
Age	−0.09	0.71	20
Clonal bone marrow plasma cells	0.09	0.74	20
Calcemia	−0.03	0.89	20
Creatinine serum level	−0.38	0.09	20
Hemoglobin serum level	0.05	0.83	20

the opportunity to shorten imaging time by removing the T1-weighted sequence from the protocol.

In our study, we did not identify a correlation between fat fraction and biological data of the extended CRAB. In case of a correlation between fat fraction assessed by T2-weighted Dixon sequence and biological data, MRI could have been used as a non-invasive tool to assess the level of clonal bone marrow plasma cells. Unfortunately, we did not demonstrate such a correlation. In our experience, diffuse bone marrow infiltration on T2-weighted Dixon images did not impair the contrast between focal lesions and bone marrow. New sequences have emerged in the diagnosis of MM and treatment follow-up, including the diffusion-weighted sequence. Indeed, invasion of the bone marrow by plasmocytes causes restricted water motion [18]. Therefore, either focal lesions or diffuse tumor cell infiltration of bone marrow appear as hyperintense on high b value diffusion-weighted images (DWI). Bone lesion conspicuity is higher on DWI with b value of 800s/mm^2 than on STIR images [19], and apparent diffusion coefficient (ADC) values have been shown to be useful for assessing disease course in MM [20,21].

In the clinical setting, other modalities such as 18-fluorodeoxyglucose (FDG) PET-CT are useful to detect focal MM lesions [22]. MRI and 18-FDG PET-CT have similar performances for the detection of focal MM lesions of the spine and pelvis [23,24]. In the future, the diagnostic value of T2-weighted Dixon whole-body MRI should be compared to that of 18-FDG PET-CT. Indeed, whole-body MRI has an increasing place in the assessment of MM spread. In a study conducted by Walker et al. involving 611 patients with MM, whole body MRI revealed more focal MM lesions than conventional whole-body x-rays in three of the most common metastatic sites for MM, including spine, pelvis and sternum [25]. As compared to whole-body multidetector computed tomography (MDCT), whole-body MRI has a higher sensitivity both for focal and diffuse pattern of bone marrow involvement and will result in upstaging MM. Moreover, the detection rate of extensive disease and the rate of bone manifestations using whole-body-MRI are higher than whole-body MDCT [26].

This study has some limitations. First, we acknowledge that we did not compare the sensitivity of T2-weighted Dixon to that of T1-weighted sequence to detect MM lesions. Such a comparison would have required a complementary study comparing the number of focal MM lesions detected on each sequence. Secondly, it is a retrospective and single-centre study, with the result that our results warrant confirmation by a prospective multicenter study. The size of our sample was too small to allow us to draw any definitive conclusions regarding the potential link between fat fraction assessed by T2-weighted Dixon and the extended CRAB data. Finally, the impact of patient's treatments on the contrast was not assessed. Yet, signal changes of focal MM lesions and of surrounding bone marrow under treatment might likely impact contrast over time. A cohort study with a larger population would be required to overcome this limitation.

In conclusion, for the assessment of myeloma focal lesions, T2-weighted Dixon fat-only images result in greater contrast between MM lesions and adjacent bone marrow than T1-weighted images, but fat fraction does not correlate with biological data of the extended CRAB. The diagnostic value of the T2-weighted Dixon in MM, and of its association with a T1-weighted sequence has to be determined. If the non-inferiority of T2-weighted Dixon sequence compared to other fat-suppressed fluid-sensitive sequences was

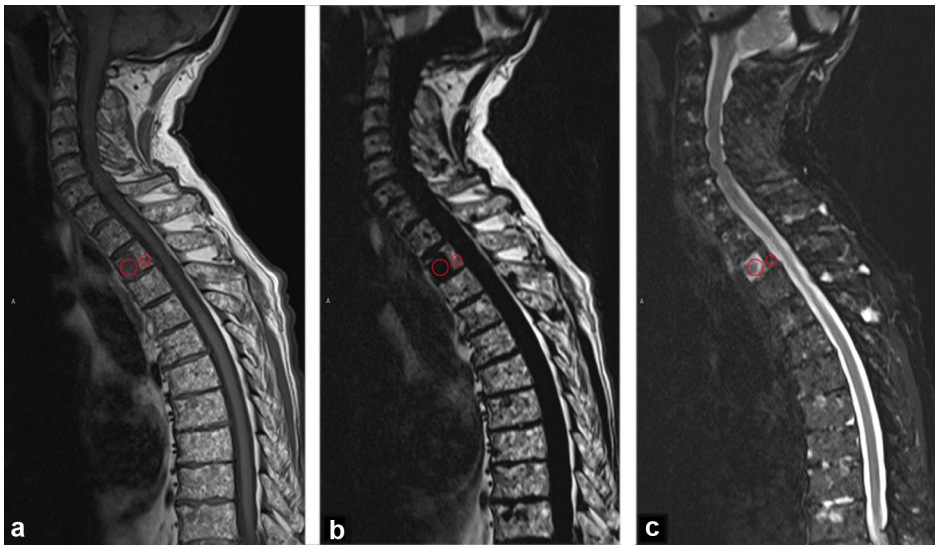

Figure 3. 81-year-old man with diffuse bone marrow infiltration and multiple focal myeloma lesions. a: On T1-weighted image in the sagittal plane, all myeloma lesions show low signal intensity; b: On T2-weighted Dixon fat-only image all myeloma lesions have no detectable signal; c: On T2-weighted Dixon water-only image all myeloma lesions have high signal intensity. For example, the lesion of the second thoracic vertebral body (large circles) has a contrast equal to 0.37 on T1-weighted, 0.96 on T2-weighted Dixon fat-only and 0.49 on T2-weighted Dixon water-only images.

demonstrated, it could become an all-in-one alternative to the classical association of T1-weighted plus another fat-suppressed fluid-sensitive sequence.

Human and animal rights

The authors declare that the work described has been carried out in accordance with the Declaration of Helsinki of the World Medical Association revised in 2013 for experiments involving humans.

Informed consent and patient details

The authors declare that this report does not contain any personal information that could lead to the identification of the patient(s).

Funding

This work did not receive any grant from funding agencies in the public, commercial, or not-for-profit sectors.

Author contributions

All authors attest that they meet the current International Committee of Medical Journal Editors (ICMJE) criteria for Authorship.

Disclosure of interest

The authors declare that they have no competing interest.

References

[1] Rajkumar SV, Dimopoulos MA, Palumbo A, Blade J, Merlini G, Mateos MV, et al. International Myeloma Working group updated criteria for the diagnosis of multiple myeloma. Lancet Oncol 2014;15:e538—48.
[2] Dimopoulos MA, Hillengass J, Usmani S, Zamagni E, Lentzsch S, Davies FE, et al. Role of magnetic resonance imaging in the management of patients with multiple myeloma: a consensus statement. J Clin Oncol 2015;33:657—64.
[3] Howe BM, Johnson GB, Wenger DE. Current concepts in MRI of focal and diffuse malignancy of bone marrow. Semin Musculoskelet Radiol 2013;17:137—44.
[4] Nakatsu M, Hatabu H, Itoh H, Morikawa K, Miki Y, Kasagi K, et al. Comparison of short inversion time inversion recovery (STIR) and fat-saturated (chemsat) techniques for background fat intensity suppression in cervical and thoracic MR imaging. J Magn Reson Imaging 2000;11:56—60.
[5] Fleckenstein JL, Archer BT, Barker BA, Vaughan JT, Parkey RW, Peshock RM. Fast short-tau inversion-recovery MR imaging. Radiology 1991;179:499—504.
[6] Del Grande F, Santini F, Herzka DA, Aro MR, Dean CW, Gold GE, et al. Fat-suppression techniques for 3-T MR imaging of the musculoskeletal system. Radiographics 2014;34:217—33.
[7] Maas M, Dijkstra PF, Akkerman EM. Uniform fat suppression in hands and feet through the use of two-point Dixon chemical shift MR imaging. Radiology 1999;210:189—93.
[8] Pezeshk P, Alian A, Chhabra A. Role of chemical shift and Dixon based techniques in musculoskeletal MR imaging. Eur J Radiol 2017;94:93—100.
[9] Reeder SB, Wen Z, Yu H, Pineda AR, Gold GE, Markl M, et al. Multicoil Dixon chemical species separation with an iterative least-squares estimation method. Magn Reson Med 2004;51:35—45.
[10] Kirchgesner T, Perlepe V, Michoux N, Larbi A, Vande Berg B. Fat suppression at three-dimensional T1-weighted MR imaging of the hands: Dixon method versus CHESS technique. Diagn Interv Imaging 2018;99:23—8.

[11] Maeder Y, Dunet V, Richard R, Becce F, Omoumi P. Bone marrow metastases: T2-weighted Dixon spin-echo fat images can replace T1-weighted spin-echo images. Radiology 2018;286:948—59.
[12] Özgen A. The value of the T2-weighted multipoint Dixon sequence in MRI of sacroiliac joints for the diagnosis of active and chronic sacroiliitis. AJR Am J Roentgenol 2017;208:603—8.
[13] Maas M, Akkerman EM, Venema HW, Stoker J, Heeten Den GJ. Dixon quantitative chemical shift MRI for bone marrow evaluation in the lumbar spine: a reproducibility study in healthy volunteers. J Comput Assist Tomogr 2001;25:691—7.
[14] Ricci C, Cova M, Kang YS, Yang A, Rahmouni A, Scott WW, et al. Normal age-related patterns of cellular and fatty bone marrow distribution in the axial skeleton: MR imaging study. Radiology 1990;177:83—8.
[15] Lecouvet FE, Whole-body M.R. imaging: musculoskeletal applications. Radiology 2016;279:345—65.
[16] Vande Berg BC, Lecouvet FE, Michaux L, Ferrant A, Maldague B, Malghem J. Magnetic resonance imaging of the bone marrow in hematological malignancies. Eur Radiol 1998;8:1335—44.
[17] Heynen B, Tamigneaux C, Pasoglou V, Malghem J, Vande Berg B, Kirchgesner T. MRI detection of radiographically occult fractures of the hip and pelvis in the elderly: comparison of T2-weighted Dixon sequence with T1-weighted and STIR sequences. Diagn Interv Imaging 2019;100:169—75.
[18] Padhani AR, Khan AA. Diffusion-weighted (DW) and dynamic contrast-enhanced (DCE) magnetic resonance imaging (MRI) for monitoring anticancer therapy. Target Oncol 2010;5:39—52.
[19] Pearce T, Philip S, Brown J, Koh DM, Burn PR. Bone metastases from prostate, breast and multiple myeloma: differences in lesion conspicuity at short-tau inversion recovery and diffusion-weighted MRI. Br J Radiol 2012;85:1102—6.
[20] Horger M, Weisel K, Horger W, Mroue A, Fenchel M, Lichy M. Whole-body diffusion-weighted MRI with apparent diffusion coefficient mapping for early response monitoring in multiple myeloma: preliminary results. AJR Am J Roentgenol 2011;196:W790—5.
[21] Padhani AR, van Ree K, Collins DJ, D'Sa S, Makris A. Assessing the relation between bone marrow signal intensity and apparent diffusion coefficient in diffusion-weighted MRI. AJR Am J Roentgenol 2013;200:163—70.
[22] Sager S, Ergül N, Ciftci H, Cetin G, Güner SI, Cermik TF. The value of FDG PET/CT in the initial staging and bone marrow involvement of patients with multiple myeloma. Skeletal Radiol 2011;40:843—7.
[23] Fonti R, Salvatore B, Quarantelli M, Sirignano C, Segreto S, Petruzziello F, et al. 18F-FDG PET/CT, 99mTc-MIBI, and MRI in evaluation of patients with multiple myeloma. J Nucl Med 2008;49:195—200.
[24] Walker RC, Brown TL, Jones-Jackson LB, De Blanche L, Bartel T. Imaging of multiple myeloma and related plasma cell dyscrasias. J Nucl Med 2012;53:1091—101.
[25] Walker R, Barlogie B, Haessler J, Tricot G, Anaissie E, Shaughnessy JD, et al. Magnetic resonance imaging in multiple myeloma: diagnostic and clinical implications. J Clin Oncol 2007;25:1121—8.
[26] Gleeson TG, Moriarty J, Shortt CP, Gleeson JP, Fitzpatrick P, Byrne B, et al. Accuracy of whole-body low-dose multidetector CT (WBLDCT) versus skeletal survey in the detection of myelomatous lesions, and correlation of disease distribution with whole-body MRI (WBMRI). Skeletal Radiol 2009;38:225—36.